Distribution of energy storage rate in area of strain localization during tension of austenitic steel

2015 IOP Conf. Ser.: Mater. Sci. Eng. 71 012055

(http://iopscience.iop.org/1757-899X/71/1/012055)

Distribution of energy storage rate in area of strain localization during tension of austenitic steel

W Oliferuk[1,2], M Maj[2] and K Zembrzycki[2]
[1]Białystok University of Technology, Białystok, 15-351, Poland
[2]Institute of Fundamental Technological Research, Warsaw, 02-106, Poland

E-mail: wolif@ippt.gov.pl

Abstract. The present work is devoted to experimental determination of the energy storage rate in the area of strain localization. The experimental procedure involves two complementary techniques: i.e. infrared thermography (IRT) and visible light imaging. The results of experiments have shown that during the evolution of plastic strain localization the energy storage rate in some areas of the deformed specimen drops to zero. To interpret the decrease of the energy storage rate in terms of micro-mechanisms, microstructural observations using electron back scattered diffraction (EBSC) were performed.

1. Introduction

When a material deforms plastically, a part of the mechanical energy w_p expended on plastic deformation is converted into heat q_d while the remainder e_s is stored within the material as an energy related to defects of crystal lattice, mainly dislocation structures,

$$e_s = w_p - q_d . \tag{1}$$

The stored energy e_s represents a change in internal energy of the deformed material and it is an essential measure of its cold-worked state. This energy was discovered in calorimetric tests performed by Taylor and Quinney [1]. Since then the part of plastic work stored in the metallic material was considered to be a constant value of about 10% of the whole plastic work. Nevertheless, further experimental studies have shown that the ratio of the stored energy to the plastic work is not constant and depends on deformation level of the tested material [2-14]. Thus a measure of energy conversion at each instant of the plastic deformation process was introduced. It is the rate of energy storage Z defined as the ratio of the stored energy increment Δe_s to the plastic work increment Δw_p:

$$Z = \frac{\Delta e_s}{\Delta w_p} . \tag{2}$$

The stored energy increment is equal to the difference between Δw_p and the increment of energy dissipated as a heat Δq_d ,

$$\Delta e_s = \Delta w_p - \Delta q_d .$$

Therefore:

$$Z = \frac{\Delta e_s}{\Delta w_p} = 1 - \frac{\Delta q_d}{\Delta w_p} . \tag{3}$$

The entire deformation process, from initial state to the fracture of the tested specimen, can be divided into two stages: homogeneous deformation and heterogeneous one. Two indicators of appearance of plastic strain localization are usually applied. They are: non-uniform temperature distribution on the specimen surface and non-uniform strain field on the opposite surface of this specimen.

In the previous works it has been shown that during heterogeneous deformation (localization of plastic strain) of polycrystalline material, the energy storage rate rapidly decreases reaching the 0 value and then becomes negative [13, 15]. But up to now, only the average value of the energy storage rate for the gauge part of deformed specimen was estimated. The questions appear: a) What is the energy storage rate distribution along the gauge length of the strained specimen during development of plastic strain localization? b) What is relation between distribution of energy storage rate and microstructure evolution of deformed material? The purpose of the present work is to answer these questions. To reach the purpose, the new method of energy storage rate determination has been designed. The method allows obtaining distribution of this quantity along the gauge length of the specimen. The obtained results are related to the texture evolution.

2. Methods

The energy storage rate can be calculated by a determination of plastic work increment Δw_p and corresponding increment of energy dissipated as heat Δq_d, see equation 3.

The method is based on the experimental procedure for simultaneous measurements of temperature, and strain distributions on the surface of tested specimen during tensile deformation. This procedure involves two complementary imaging techniques: CCD camera and infrared thermography (IRT). In order to determine the strain distribution, markers in form of graphite dots were plotted on one surface of the specimen. In this way, the surface was divided into sections, whose sizes are specified by the distance between the dots (Figure 1).

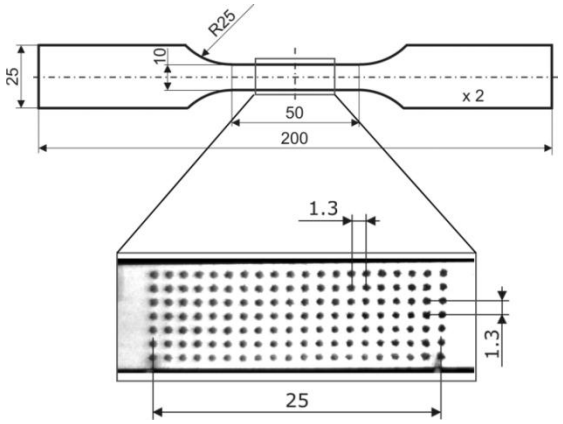

Figure 1. The graphite dots on the gauge part of the specimen and its shape and dimensions.

Displacements of the dots were recorded by means of CCD camera during deformation process. Taking into account the reference distance l_0 between the centers of the dots and recording distance between these centers as a function of deformation time $l(t,y_n)$, the true local strain $\varepsilon_y(t,y_n)$ in the direction of tension was calculated:

$$\varepsilon_y(t,y_n) = ln\left(\frac{l_y(t,y_n)}{l_0}\right), \tag{4}$$

where y_n is the vertical coordinate of the centre of section n.

The true stress σ_y was determined dividing the load by the current cross-sectional area of the specimen corresponding to the given section. Assuming that a dependence of Young's modulus *E* on strain is negligibly small, local plastic strain $\varepsilon_y^p\left(t,y_n\right)$ was obtained from the following formula:

$$\varepsilon_y^p\left(t,y_n\right)=\varepsilon_y\left(t,y_n\right)-\frac{\sigma_y\left(t,y_n\right)}{E}. \tag{5}$$

The strain and stress distributions along the axis of the tested specimen were used to calculate surface distribution of specific plastic work.

$$w_p\left(t,y_n\right)=\frac{1}{\rho\left(t,y_n\right)}\int_0^{\varepsilon_y^p\left(t,y_n\right)}\sigma_y\left(t,y_n\right)\cdot d\varepsilon_y^p, \tag{6}$$

where $\rho\left(t,y_n\right)=\frac{m_s}{V\left(t,y_n\right)}$ is the current mass density of a particular section,

$m_s=const=\rho_0\cdot V_0=\rho\left(t,y_n\right)\cdot V\left(t,y_n\right)$ is mass of a section and $V\left(t,y_n\right)$ is the current volume of particular section.

The energy dissipated in the form of heat causes an increase in the temperature of the specimen. This increase depends on the strain rate. In the area of the strain localization, the distribution of strain rate is not uniform. This heterogeneity is manifested by a non-uniform temperature field on the specimen surface. The temperature field during deformation process was recorded by means of the IR thermography system and the average temperature $T\left(t,y_n\right)$ as a function of time for each *n*-th section along the axis of the specimen was determined. Such a selection of positions of sections allows avoiding the influence of the specimen edges on the measured temperature values. The initial size of each, considered section is identified by the distance between the centres of the dots and the thickness of the specimen. Thus, the initial volume V_0 of each section was equal to $\left(1.3\times1.3\times2\right)mm^3$ and the initial cross-section S_0 was $\left(1.3\times2\right)mm^2$. Dimensions of the sections were changing during the tensile process. These changes were determined by tracking dot centres in the visible range by means of the CCD camera. All these data have been used to calculate the heat $\Delta q_d\left(t,y_n\right)$ generated during time interval Δt in $n-th$ section. The interval Δt is the reciprocal of the taking frequency.

In order to avoid the influence of the heat convection phenomenon, the displacement rate $2000\,mm/min$ was chosen. Nevertheless, despite the relatively high displacement rate the deformation process was non-adiabatic mainly due to the heat transport to the grips of the testing machine. Thus, taking in account the phenomena considered above and the heat expended for compensation of drop in temperature caused by the thermoelastic effect, the heat $\Delta q_d\left(t,y_n\right)$ generated during time Δt in $n-th$ section has been calculated according to the following formula:

$$\begin{aligned}\Delta q_d\left(t,y_n\right)=c_w\cdot\Delta T\left(t,y_n\right)+\frac{\alpha T\left(t,y_n\right)\Delta\sigma_y\left(t,y_n\right)}{\rho\left(t,y_n\right)}+\\ +\frac{S_{n/n+1}\left(t,y_n\right)\cdot\lambda\cdot\Delta t}{\rho_0\cdot V_0}\cdot\left[\frac{T\left(t,y_n\right)-T\left(t,y_{n+1}\right)}{y_{n+1}-y_n}\right]+\\ +\frac{S_{n/n-1}\left(t,y_n\right)\cdot\lambda\cdot\Delta t}{\rho_0\cdot V_0}\cdot\left[\frac{T\left(t,y_n\right)-T\left(t,y_{n-1}\right)}{y_n-y_{n-1}}\right],\end{aligned} \tag{7}$$

where α is the coefficient of linear thermal expansion, $T(t, y_n)$ is the mean absolute temperature of the considered section, $\Delta\sigma_y(t, y_n)$ is the increase in the stress during subsequent time intervals Δt, λ is the coefficient of thermal conductivity, c_w is the specific heat and V_0 is a volume of considered section. $S_{n/n+1}(t, y_n)$ and $S_{n/n-1}(t, y_n)$ are cross-section areas between neighbouring sections $n/n+1$ and $n/n-1$.

The first component of equation 7 expresses the heat needed to rise the temperature of a unit mass of the tested material by ΔT. The second describes the heat expended for compensation of the temperature drop due to the thermoelastic effect. The third and fourth components, according to the Fourier's law, take into account the heat transfer between given section n and its neighbours $n/n+1$ and $n/n-1$, respectively. It is worth to notice that the Fourier's law refers to a heat flux. Thus, in order to determine the heat related to a mass unit, the heat flux should be divided by the mass of the section and multiplied by Δt and by $S_{n/n+1}(t, y_n)$ or $S_{n/n-1}(t, y_n)$, respectively.

Adding up the heat increments $\Delta q_d(t, y_n)$ in the successive time intervals, the time dependence of the energy dissipated as heat $q_d(t, y_n)$ for each tested section has been obtained. The energy storage rate for a particular section is defined as

$$Z = 1 - \frac{\Delta q_d(t, y_n)}{\Delta w_p(t, y_n)}. \tag{8}$$

During non-uniform deformation in the equal time intervals Δt, the increments of plastic work Δw_p are not equal. Thus, Δq_d was determined for equal increments of Δw_p. In further analysis $\Delta w_p = 2\ J/g$ was taken. Such value was selected in order to reduce the dispersion of increments' ratio $\frac{\Delta q_d}{\Delta w_p}$. Having obtained $w_p(t, y_n)$ and $q_d(t, y_n)$ for the considered sections and using the procedure mentioned above the distribution of the energy storage rate was determined.

3. Experiments and results

Experiments were performed on austenitic stainless steel (304L). From the sheets of annealed material the specimens for tensile testing were cut out using electro-spark machining. In order to remove the technological surface layer, the specimens were electropolished. Optical metallographic and TEM observations of tested material indicated complete recrystallization and average grain size about 50 μm. The dislocation density in the specimens before deformation was low; dislocations were randomly distributed in the matrix and in the grain boundaries, and no regular dislocation arrangements were observed. Grains were randomly oriented (Figure 2).

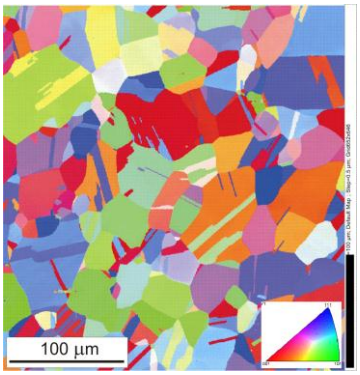

Figure 2. Distribution of grain orientation in the initial state obtained by EBSD technique.

All specimens were strained using an MTS 858 testing machine. During the tension the displacement rate was controlled and equal to $2000\,mm/min.$ For such displacement rate and given geometry of the specimen (see Figure 1) the corresponding mean value of strain rate was equal to $6.6 \cdot 10^{-1} s^{-1}$.

In the course of deformation process the infrared and visible range image sequences were recorded simultaneously. The experimental setup is presented in Figure 3.

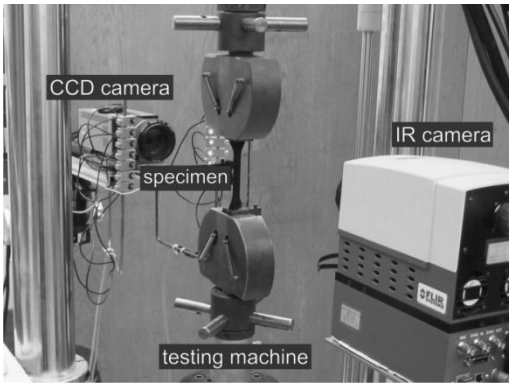

Figure 3. Experimental setup for simultaneous measurement of displacement and temperature fields.

The taking frequency of both cameras was equal to 538 *Hz*. Such frequency was selected in order to take into account the heat transfer between neighbouring sections. Simultaneously, the straining force as a function of time t was measured. The analysis of the displacement fields (based on markers tracking) and the assignment of them to the appropriate temperature distributions were performed using MATLAB software.

From the experimental data, tensile curves for selected local sections: A, B, C, D, E, lying on the axis of specimen, were calculated (Figure 4).

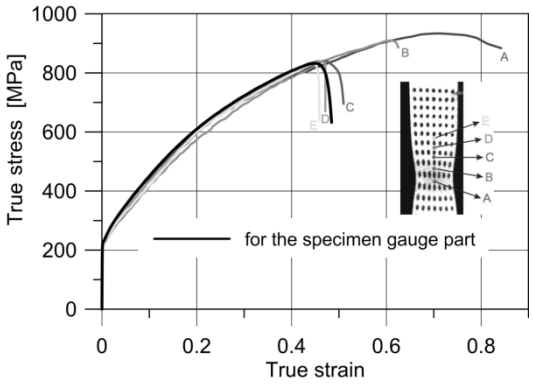

Figure 4. Stress-strain curves for selected sections of the specimen.

It is seen that with an increase in strain, the individual sections of the specimen stop to deform, whereas others are still deforming. It is result of the localization of plastic deformation. On the basis of the stress-strain dependences, the plastic work as a function of time for the selected sections lying on the specimen's axis were calculated (Equation 6).

From the surface temperature field, the distribution of energy dissipated as heat along the specimen axis was determined using a local form of heat equation (Equation 7). Then, using Equation 3 the energy storage rate Z for each of the considered sections was obtained. The results, as a function of true strain, are presented in Figure 5. Results obtained for different sections are marked by different symbols with different gray intensity, corresponding to stress-strain curves shown in Figure 5.

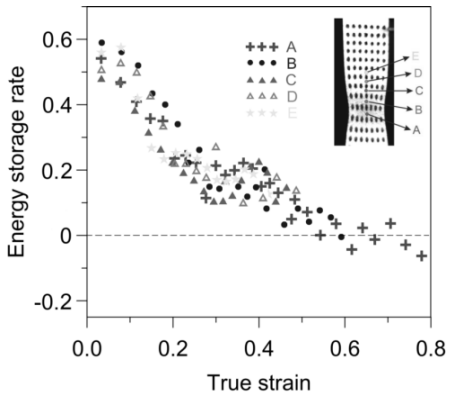

Figure 5. Energy storage rate as a function of true strain for selected sections of the specimen.

It is seen that the energy storage rate decreases with strain for all considered sections. During the evolution of plastic strain localization some sections cease to deform, which causes a stop in the energy storage process in this region, whereas the energy storage rate in the other sections (where deformation still proceeds) drops to zero. It has been shown [15] that for austenitic steel the zero value of the energy storage rate corresponds to the point of Considèr stability criterion. Thus, $\frac{\Delta e_s}{\Delta w_p} = 0$ can be treated as the plastic instability criterion based on energy conversion. A confirmation of obtained negative values of Z needs further studies. Negative values of this quantity could be explained by a release of the energy stored in previous deformation stages.

In order to find microscopic interpretation of obtained results, the study of evolution of the crystallographic orientations during the deformation process were performed using Electron Back Scattering Diffraction (EBSD) technique.

To obtain the crystallographic orientation maps for different levels of plastic deformation, three specimens were strained to the different values of strain: 0.3, 0.4 and 0.8. These values correspond to macroscopically uniform deformation, the onset of strain localization and state just before fracture, respectively. Then, the orientation maps were obtained for the selected areas of deformed specimens. The maps are shown in Figures 6-8. One can see that from the onset of plastic strain localization (Figure 7) the amount of mechanical twins increases. It means that the contribution of twinning in deformation process is growing.

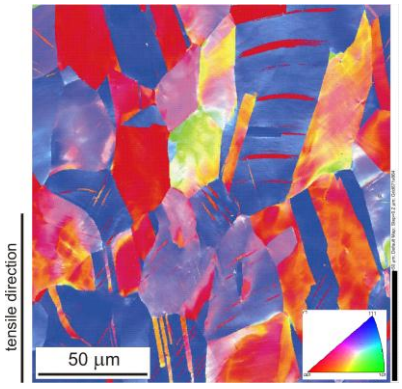

Figure 6. EBSD image for macroscopically homogeneous deformation.

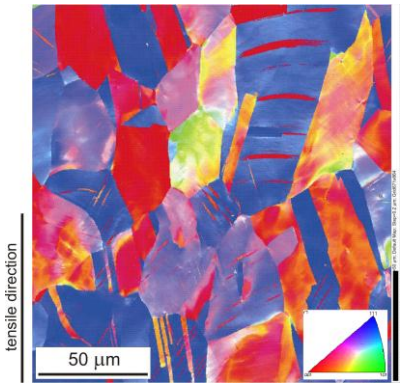

Figure 7. EBSD image for the onset of plastic strain localization.

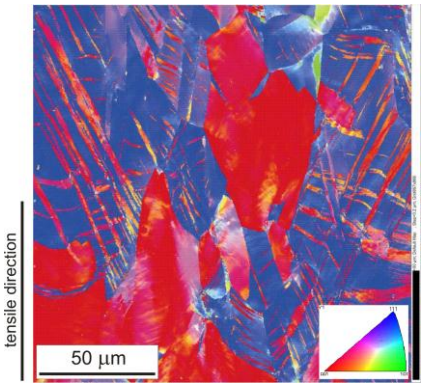

Figure 8. EBSD image for advanced localization of plastic strain (just before fracture).

In Figures 6-8 a noticeable trend in the evolution of the orientation of individual grains in direction of two dominant texture components is observed. It is seen that the development of strain localization is accompanied by further rotation of individual grains in the direction of two texture components. Rotation of grains proceeds in such a way, that the {111} type planes become parallel to the planes of maximum shear stress. The angle between the trace of these planes and the tension direction is about 40^0. The above analysis shows that in the necking zone, just before the fracture (see Figure 8), the macroscopic shear of the localized area is possible without change of a crystallographic plane. In other words, the conditions for the crystallographic shear banding are created [16]. This corresponds to the loss of stability of the plastic deformation. The presented preliminary results have shown that the zero value of the energy storage rate may be treated as a criterion of plastic instability. An interpretation of such criterion in terms of microstructure evolution requires further studies.

4. Conclusions

Experimental method of determination of energy storage rate distribution in the area of heterogeneous deformation has been proposed.

It has been shown, that in the plastic strain localization area material reaches the state, where energy storage rate reaches the 0 value and then becomes negative. This means that the material loses an ability to store the energy, though energy supply the internal energy of the specimen decreases. Thus, the 0 value of the energy storage rate could be regarded as the plastic instability criterion based on the energy conversion.

On the basis of microstructure observation it is believed that 0 value of energy storage rate corresponds to the state in which only two dominant components of the texture appear, creating conditions to crystallographic shear-banding.

References

[1] Taylor G and Quinney H 193) The latent energy remaining in a metal after cold working *Proc R Soc Lond* **143** 307-326
[2] Bever M B, Holt D L and Titchener A L 1973 The stored energy of cold work *Prog Mater Sci*, Pergamon Press **17** 23-58
[3] Oliferuk W, Gadaj S P and Grabski M W 1984 Energy storage during the tensile deformation of Armco iron and austenitic steel *Mater Sci Eng* **70** 131-141
[4] Chrysochoos A and Maisonneuve O 1985 Energy balance for elastic plastic deformation at finite strain *C R Acad Sci* **300** 985-990
[5] Oliferuk W, Świątnicki W and Grabski MW 1993 Rate of energy storage and microstructure evolution during the tensile deformation of austenitic steel *Mater Sci Eng A* **161** 55-63
[6] Chrysochoos A, Maisonneuve O, Martin G, Caumon H and Chezeaux JC 1989 Plastic and dissipated work and stored energy *Nucl Ebg Des* **114** 323-333
[7] Oliferuk W, Świątnicki W and Grabski MW 1995 Effect of grain size on the rate of energy storage during the tensile deformation of austenitic steel *Mater Sci Eng A* **197** 49-58

[8] Oliferuk W, Korbel A and Grabski MW 1997 Slip behaviour and energy storage process during uniaxial tensile deformation of austenitic steel *Mater Sci Eng A* **224-226** 1122-1125
[9] Rittel D 1999 On the conversion of plastic work to heat during high strain rate deformation of glassy polymers *Mech Mat* **31** 131-139
[10] Chrysochoos A and Louche H 2000 An infrared image processing to analyse the calorific effects accompanying strain localization *Int J Eng Sci* **38** 1759-1788
[11] Hodowany J, Ravichandran G, Rosakis A J and Rosakis P 2000 Partition of plastic work into heat and stored energy in metals *Exp Mech* **40** 113-123
[12] Oliferuk W, Korbel A and Bochniak W 2001 Energy balance and macroscopic strain localization during plastic deformation of polycrystalline metals *Mater Sci Eng A* **319-321** 250-253
[13] Oliferuk W, Maj M and Raniecki B 2004 Experimental analysis of energy storage rate components during tensile deformation of polycrystals *Mater Sci Eng A* **374** 77-81
[14] Oliferuk W and Maj M 2004 Effect of pre-strain direction on energy storage process during tensile deformation of polycrystal *Mater Sci Eng A* **387-389** 218-221
[15] Oliferuk W and Maj M 2007 Plastic instability criterion based on energy conversion *Mater Sci Eng A* **462** 363-366
[16] Paul H and Driver JH 200) Deformation structure and texture transformations in twinned fcc metals: Critical role of micro- and macro- scale shear bands *Mater Sci Forum* **550** 521-526